

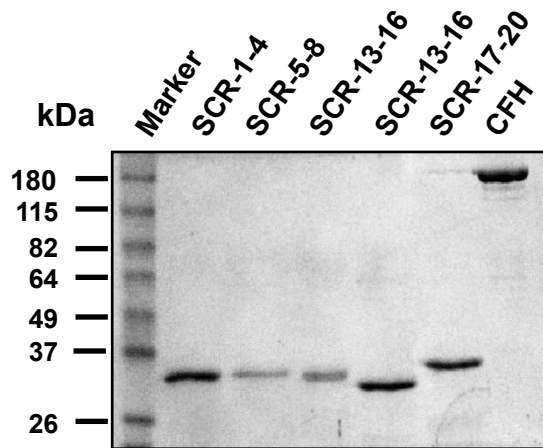
Supplementary tables and figures (Gurjar et al.)

Table S1. *Primers used for the construction of truncated CFH fragments*

Mutant	Primer	Sequence ^a
SCR 1-4	Forward	5'-CATG CCATGGC CAGAAGATTGCAATGAACTTCCTCCAAG-3'
	Reverse	5'-CCG CTCGAGT GATTTTTCTTCACATGAAGGCAACG-3'
SCR 5-8	Forward	5'-CATG CCATGGC CATGTGATAATCCTTATATTCCAAATGGTG-3'
	Reverse	5'-CCG CTCGAG AGATTTAATGCACGTGGGTTGAGC-3'
SCR 9-12	Forward	5'-CATG CCATGGC CATGTGATATCCCAGTATTTATGAATGC-3'
	Reverse	5'-CCG CTCGAG CTTCTTAAGTTTATCTATTGCCACAC-3'
SCR 13-16	Forward	5'-CATG CCATGGC CATGCAAATCATCAAATTTAATTATACTTGAG-3'
	Reverse	5'-CCG CTCGAG ATCTGTTTTTATGCATGATGCAGGGTG-3'
SCR 17-20	Forward	5'-GGAATT CCATATG TGTCTCAGTTTACCTAGCTTTGAAAATG-3'
	Reverse	5'-CCG CTCGAG TCTTTTTGCACAAGTTGGATACTCC-3'

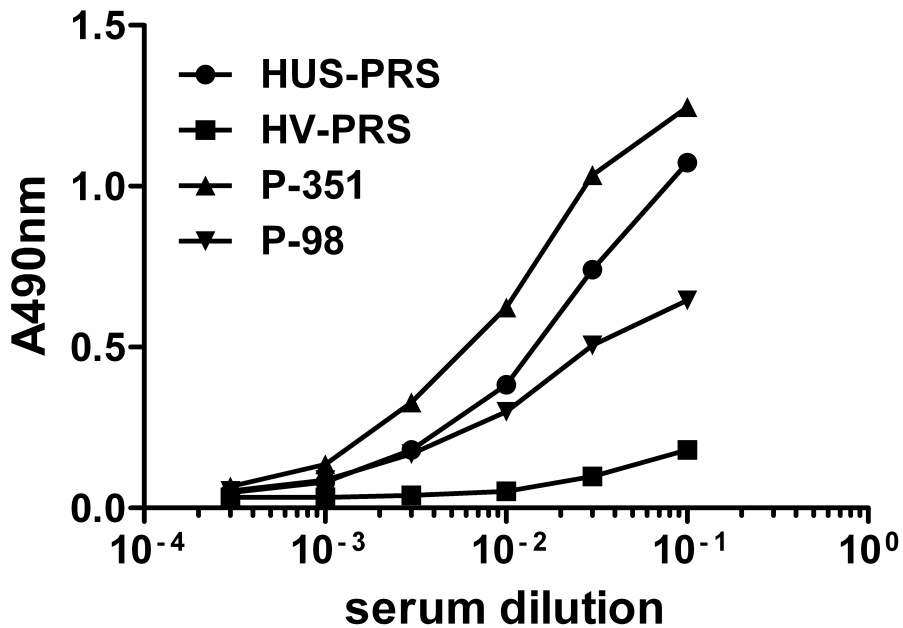
^aThe restriction sites in the primers are indicated by boldface.

Fig. S1. SDS-PAGE analysis of CFH and its truncation mutants



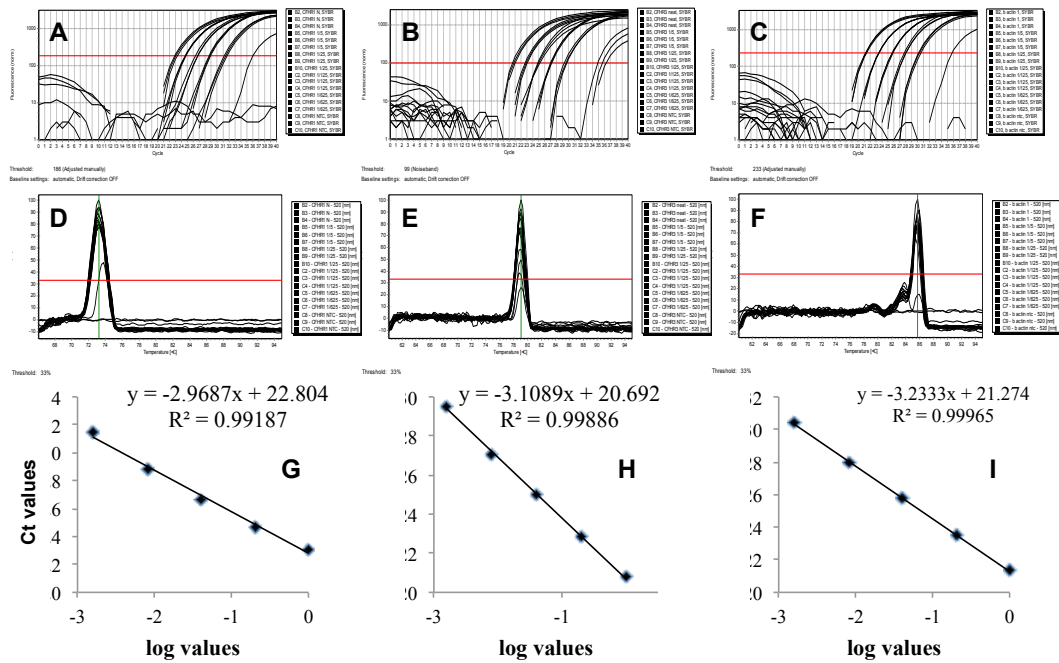
Purified CFH and its mutants were subjected to electrophoresis through a 10% SDS-PAGE gel under reducing conditions and stained with Coomassie Blue.

Fig. S2. *Immunoassay of serum anti-CFH autoantibodies*



Serum anti-CFH antibody levels were estimated by ELISA. Examples of the titration of various sera on CFH-coated microplates are shown. Pooled reference serum from aHUS patients (HUS-PRS), pooled reference serum from healthy volunteers (HV-PRS), and two individual aHUS patient sera are shown. The anti-CFH antibody concentration in the HUS-PRS shown was 9600 arbitrary units (AU)/ml for reference purposes, while the calculated anti-CFH antibody concentrations were 47748 AU/ml in P-351, 2041 AU/ml in P98, and <200 AU/ml in HV-PRS.

Fig. S3. Quantitative PCRs for the human *CFHR1*, *CFHR3*, and *BETA-ACTIN* genes



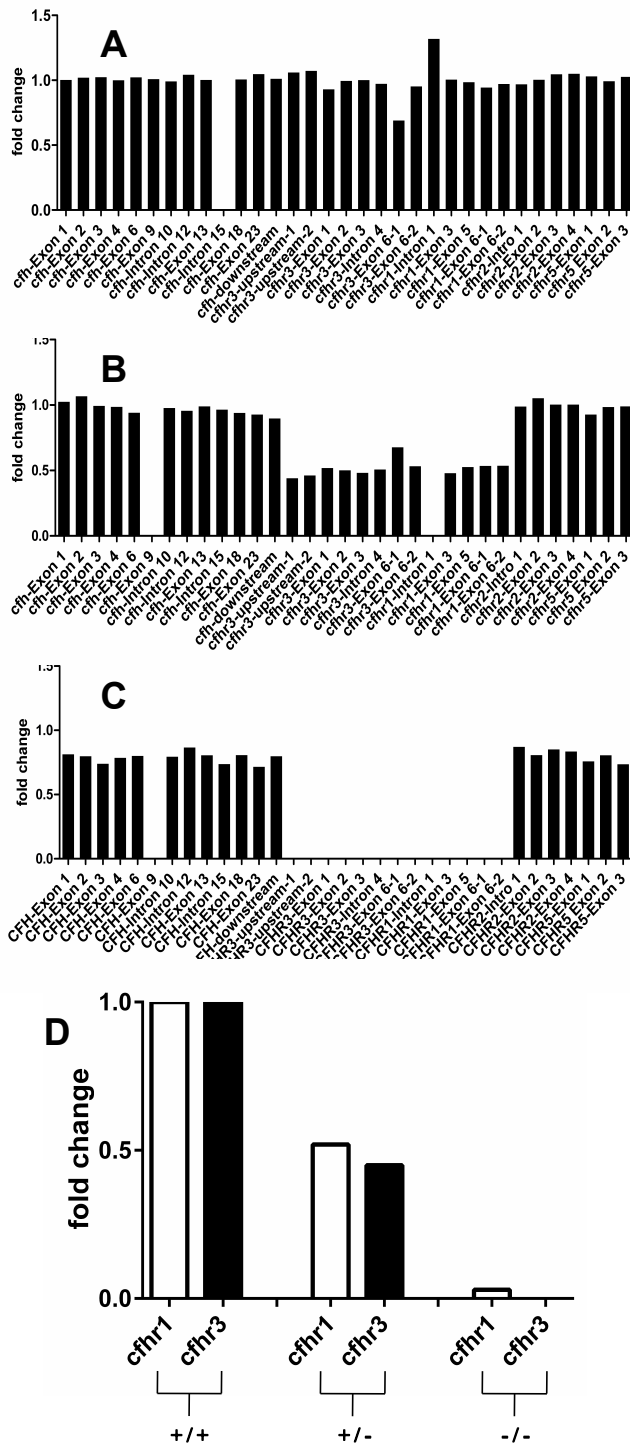
(A-C) Amplification plots using *CFHR1* (A), *CFHR3* (B), and *BETA-ACTIN* (C) gene primers in triplicates using titrating amounts of genomic DNA (125 ng, 25 ng, 5 ng, 1 ng and 0.2 ng).

(D-F) Melting curves for *CFHR1* (D), *CFHR3* (E), and *BETA-ACTIN* (F) reactions above, indicating single amplified products.

(G-I) Standard curves of qPCR reactions done in A-C above, for *CFHR1* (G), *CFHR3* (H), and *BETA-ACTIN* (I) genes, showing reliable quantification with $R^2 > 0.99$.

Fig. S4. MLPA and qPCR analyses for *CFHR1*, *CFHR3*, and *BETA-ACTIN*

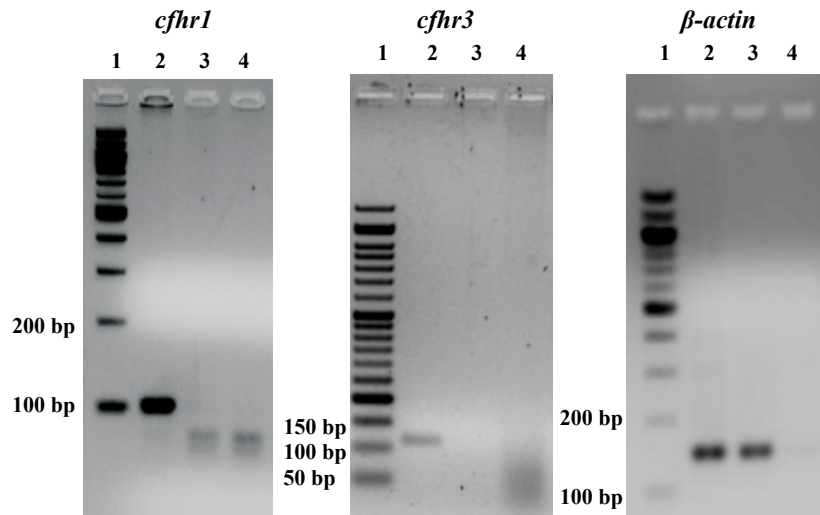
genes



(A-C) MLPA analysis of the *CFH-CFHR* locus in genomic DNA samples from individuals +/+ (A), +/- (B) or -/- (C) for *CFHR1* and *CFHR3*, shown as fold-changes with respect to *CFH* exon 1 in the +/+ sample.

(D) Results of qPCR analysis for *CFHR1* and *CFHR3* genes normalized respect to *BETA-ACTIN* in DNA samples +/+ (D), +/- (E) and -/- (F) as used in A-C, shown as fold-changes with respect to the +/+ (HV) sample.

Fig. S5. End-point PCR for determination of the *cfhr1* and *cfhr3* genotype in human genomic DNA



Standard PCR was carried out on genomic DNA for *CFHR1*, *CFHR3* and *BETA-ACTIN* as shown, and products were electrophoresed on a 2.5% agarose gel. In all gels, *lane 1*: markers, *lane 2*: +/+ *CFHR1* and *CFHR3* DNA, *lane 3*: -/- *CFHR1* and *CFHR3* DNA, *lane 4*: no-template control, showing absence of *CFHR1* and *CFHR3* bands in the -/- genotype. Expected amplicon sizes for *CFHR1*, 100 bp, for *CFHR3*, 120 bp, and for *BETA-ACTIN*, 150 bp.